Supplemental Figure 1. TRPC5 antibody and knockdown validation studies.

a) Western blot from TRPC5-GFP or TRPC6-GFP transfected HEK cell lysates shows the specificity of the antibody for TRPC5. The same blot was probed with the GFP antibody as a positive control. **b)** Western blots from brain lysates from TRPC5 KO versus WT mice show that TRPC5 is only detected in WT tissue. This confirms the specificity of this newly developed TRPC5 antibody. **c)** TRPC5 labeling is noted in podocyte cell bodies and primary processes (arrowheads) in sections from WT but not TRPC5 KO kidneys. The podocyte-specific marker podocin has a similar appearance (arrowheads). Some non-specific background staining is noted in both WT and KO kidney sections stained with the TRPC5 antibody. **d)** qPCR for the validation of podocyte TRPC5 depletion. This experiment shows that lentivirally delivered TRPC5 shRNA results in > 75% depletion of TRPC5 mRNA in podocytes.

Supplemental Figure 2. ML204 blocks LPS-stimulated TRPC5 channel activity.

a) Whole cell recordings in HEK cells transfected with TRPC5-GFP show that LPS activates a current with the characteristic doubly rectifying I-V curve, which is abrogated by the application of ML204 (3 μM). **b)** Statistical analysis confirms that ML204 can efficiently block inward (V_m = -100 mV) and outward TRPC5 currents (V_m = + 100 mV) induced by LPS (n = 5 cells, $P < 0.05$, ANOVA). **c)** Representative single channel recordings in the outside-out configuration show the effect of LPS as compared to Ang II (positive control)(Tian et al., 2010) on TRPC5 single channel activity (P_o).

Supplemental Figure 3. ML204 protects from PS- and LPS-mediated remodeling of the actin cytoskeleton.

a) PS (300 μg/ml) induces loss of actin stress fibers and synaptopodin staining compared to control, but this phenotype is reversed with progressively greater efficiency by escalating doses of ML204 (3-30 μM). **b)** Quantification of dose responsive protection by ML204 in PS-treated podocytes (n=90 images/condition, $P<0.00001$, ANOVA). **c)** LPS (100 μg/ml) induces loss of actin stress fibers compared to control, but this phenotype is reversed by ML204 (10 μM). **d)** Quantification of stress fiber protection by ML204 in LPS-treated podocytes (n=90 images/condition, $P<0.001$, ANOVA).

Supplemental Figure 4. ER Ca^{2+} store depletion does not affect the amplitude of peak Ca^{2+} transients induced by Cch in isolated glomeruli.

a) Averaged response from Cch (100 μM) induced Ca^{2+} transients in Fura-2 loaded podocytes on isolated WT mouse glomeruli (n=11 glomeruli). **b)** Pre-treatment with Thapsigargin (Tg, 10 μM, n=12 glomeruli) to deplete internal stores did not affect the peak response induced by CCh, but did induce a response similar to the plateau responses observed after Cch stimulation in Figure 6a. **c)** No significant difference (n.s.) was observed in the peak average responses from CCh versus CCh + Tg in podocytes on isolated glomeruli, suggesting that the Cch-mediated peak calcium response is mediated by influx of Ca^{2+} through a channel in the plasma membrane.

Supplemental Movie. Confocal imaging of LifeAct-infected podocytes treated with PS (left panel) demonstrates the dynamics of cytoskeletal remodeling in real time including a) increased ruffling and lamellipodia activity, followed by b) loss of actin stress fibers, and ultimately c) an involution of the cell onto itself, leading to the accumulation of intensely fluorescent aggregates. This response is abrogated in Lifeact infected podocytes treated with ML204 in the presence of PS (right panel).

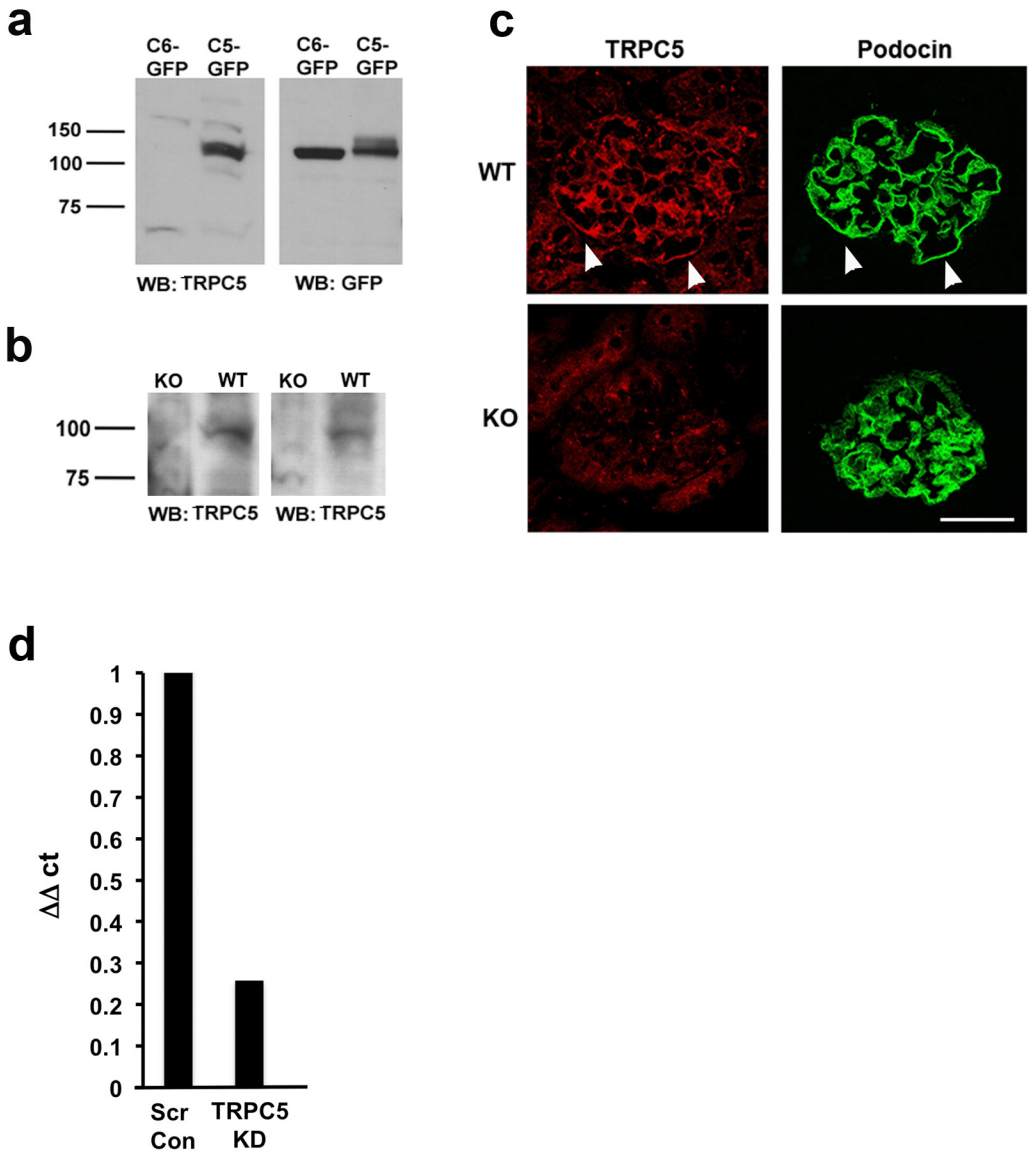

Supplemental Figure 1

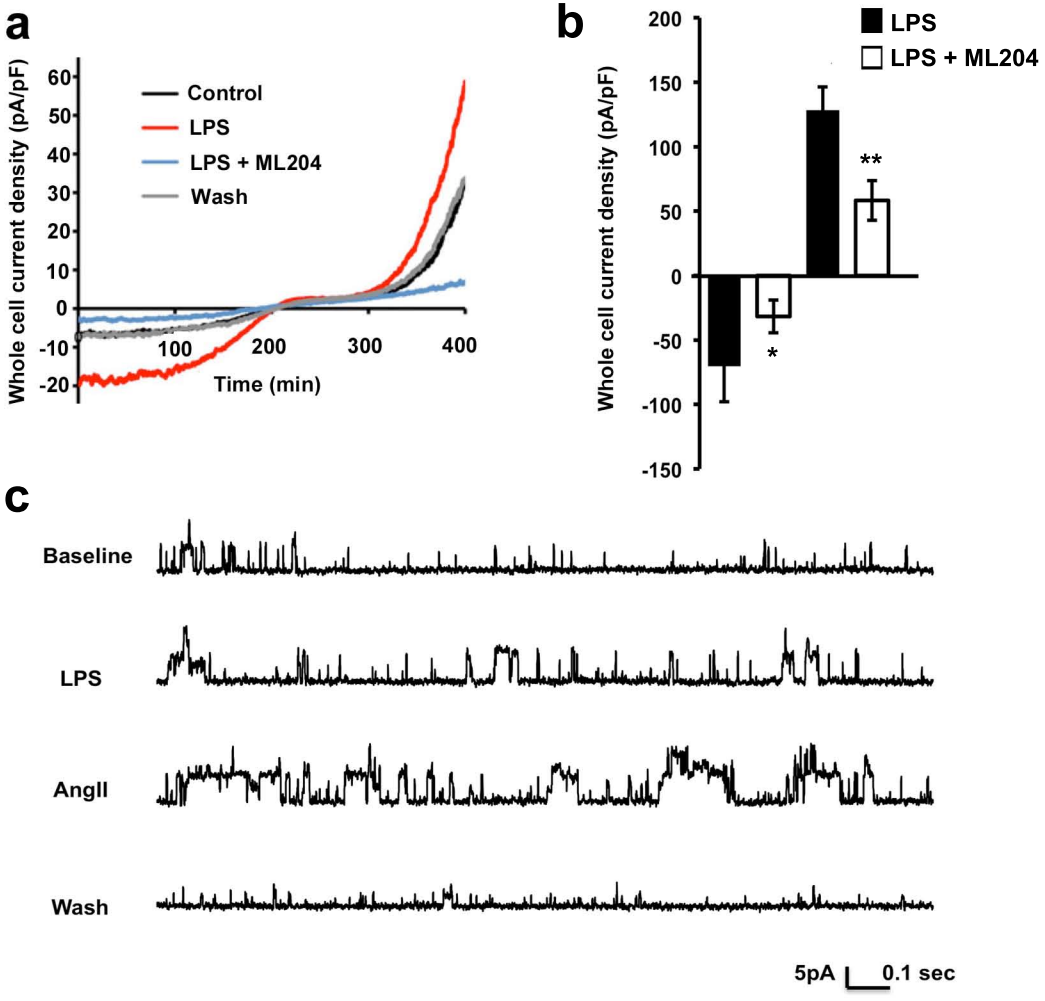

Supplemental Figure 2

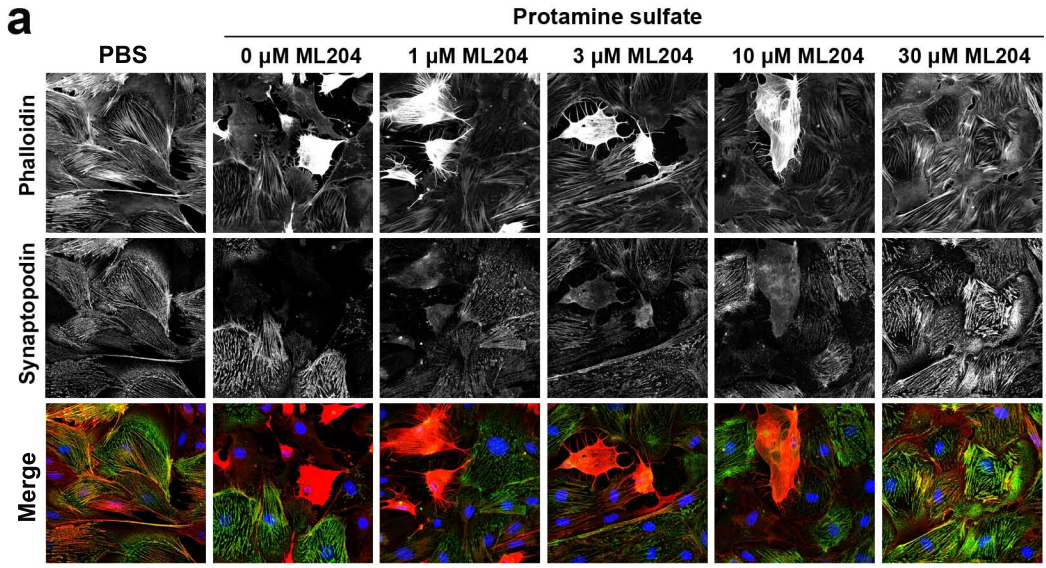

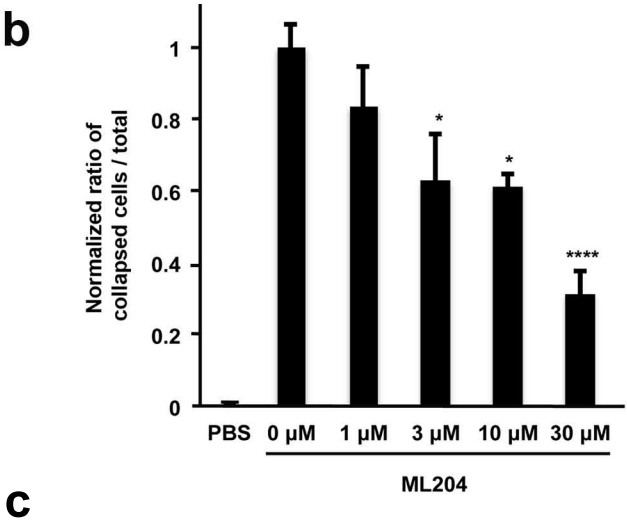

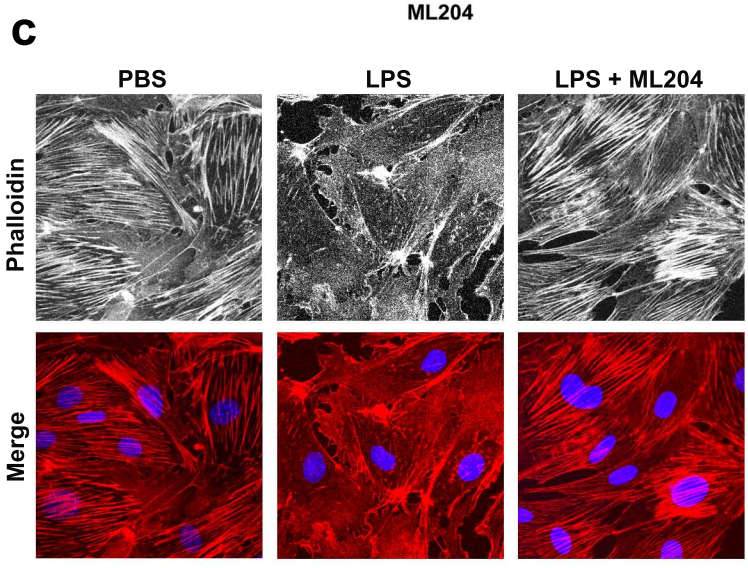

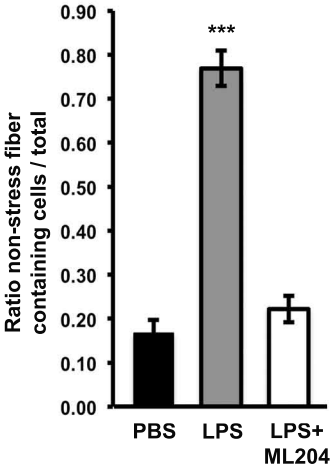

Supplemental Figure 3

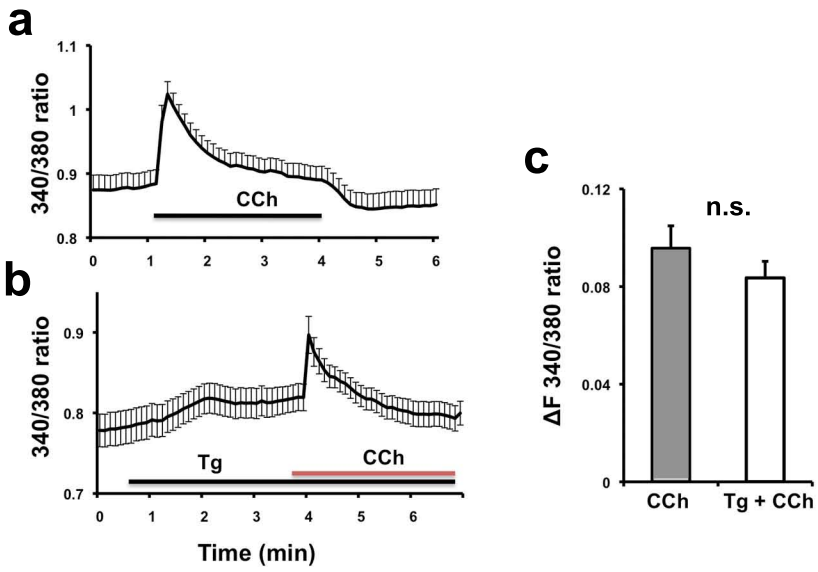

Supplemental Figure 4